JOURNAL OF THE ROYAL SOCIETY Interface

rsif.royalsocietypublishing.org

Research

Cite this article: Hashemi SM, Sens P, Mohammad-Rafiee F. 2014 Regulation of the membrane wrapping transition of a cylindrical target by cytoskeleton adhesion. *J. R. Soc. Interface* **11**: 20140769.
http://dx.doi.org/10.1098/rsif.2014.0769

Received: 15 July 2014
Accepted: 22 August 2014

Subject Areas:
biophysics, biomechanics, biomathematics

Keywords:
membrane deformation, phagocytosis, membrane–particle adhesion

Author for correspondence:
Farshid Mohammad-Rafiee
e-mail: farshid@iasbs.ac.ir

Royal Society Publishing

Regulation of the membrane wrapping transition of a cylindrical target by cytoskeleton adhesion

Seyed Mahmoud Hashemi[1], Pierre Sens[2] and Farshid Mohammad-Rafiee[1]

[1]Department of Physics, Institute for Advanced Studies in Basic Sciences (IASBS), Zanjan 45137-66731, Iran
[2]Gulliver UMR 7083, CNRS-ESPCI, 10 rue Vauquelin, 75231 Paris Cedex 05, France

The adsorption of external objects to the cell membrane often triggers cellular responses involving large deformations. In phagocytosis, upon contact with the target, the cell creates large extensions that wrap around the target and ultimately lead to its engulfment. Although active force generation, in particular by actin polymerization, is required for completion of this process, the elastic deformation of the cell membrane upon adhesion to an external object might play an important part in its initiation. In this paper, the elastic deformation of a bilayer owing to the binding of a cylindrical object is studied, taking into account the membrane bending rigidity and the surface tension, the membrane adhesion to both the external target and inner cytoskeleton. The problem is studied within the framework of the Helfrich–Hamiltonian and using force balance relations and the proper boundary conditions that are related to the adhesion energy coefficients. It is shown that membrane wrapping around the target may be a continuous or abrupt transition upon increasing the target binding energy, depending on the value of the parameter. The degree of wrapping and the shape of the membrane in the vicinity of the object are computed numerically, and analytical expressions are given for the boundaries separating the different wrapping regimes in the parameter space.

1. Introduction

One of the essential features of living cells is the presence of a soft, thin, flexible structure called the membrane that separates the cell from its surroundings and its components from each other [1]. The membrane can be deformed significantly owing to its interaction with external objects. The deformability of a biological membrane is of vital importance to many essential life processes such as endocytosis, exocytosis and cell crawling. The mechanical properties of membranes play a crucial role in active and passive deformations [2]. While understanding some aspects of deformability of a biological membrane requires the details of its chemical components, there are quite a number of processes that involve significant conformational changes in the membrane [3]. For example, consider the phagocytosis process in which eukaryotic cells such as macrophages and neutrophils bind and engulf external materials about 1 μm in diameter [4]. Furthermore, normally, biological membranes are attached tightly to the cytoskeleton of cells. The local cortex dynamics has an important effect on the local deformability of the membrane [5].

The elastic description of the membrane response to mechanical stresses has been developed over the past decades. Because the thickness of the biological membrane (a few nanometres) is much smaller than the typical lengthscale of the membrane, the shell elastic theory [6] has been used widely for describing the shape of a membrane [7,8]. In this limit, it is possible to define a stress tensor in order to study the deformation of the system [9]. It is convenient to interpret the stress tensor in terms of the phenological Helfrich–Hamiltonian that is firstly introduced in [10]. This description of membrane deformations is suitable when the radius of the membrane curvature is much larger than the

characteristic length of the system which is set by the membrane thickness [11]. In this framework, the adsorption of a single or multiple cylindrical object(s) to a flat membrane has been studied [12,13]. In addition, it is well known that the cytoskeletal networks have an important effect on the adhesion of a membrane to a substrate and/or to other cells [1,14,15].

Motivated by aforementioned problems, here we set out to consider a biological membrane, which was originally flat, to which a cylindrical object is adhered. Naturally, the cytoskeleton of the cell is attached to the membrane and makes its deformation more difficult. The aim of this paper was to show the effect of the cytoskeleton on the deformation of the flat membrane owing to the adsorption of a cylindrical colloid. The rest of paper is organized as follows: §2 describes the model. After a general introduction of the model, we derive the shape equations of the membrane, the relation between the adhesion and the membrane shape, and the proper boundary conditions of the problem. In §3, we present the results, and finally in §4, we conclude the paper.

2. The model

Owing to the adhesion of the particle to the membrane, one expects to see a deformation on the membrane. One further expects that the deformation should vanish at a finite distance from the particle (called r_s) owing to membrane/cytoskeleton adhesion. In figure 1, the geometry of the problem is shown schematically. As can be seen in figure 1, one can distinguish three parts in the membrane, the *cap* in which the membrane engulfs the object, the *free* part, where the membrane does not have interaction with neither the object nor the cytoskeleton and the *tail* part in which the membrane is adhered to the cytoskeleton.

The total energy of the problem has the following contributions: (i) the total adhesion energy, (ii) the total elastic deformation energy of the adhered membrane to the object and (iii) the total elastic deformation energy of the free membrane. We assume that the equilibrium shape of the membrane can be obtained as a balance of the mentioned energy contributions. The total adhesion energy per unit length of the cylinder, E_{ad}, is written as

$$E_{\mathrm{ad}} = -2wa\alpha + 2w_s r_s, \tag{2.1}$$

where a is the radius of the cylinder, w and w_s denote the cylinder–membrane and the cytoskeleton–membrane adhesion energy, respectively, and α shows the amount of engulfment of the particle (figure 1). The elastic energy per unit length of the membrane in the *cap* part can be calculated using the Helfrich energy [10] as

$$E_{\mathrm{cap}} = \kappa\frac{\alpha}{a} + 2\sigma\alpha a\left(1 - \frac{\sin\alpha}{\alpha}\right), \tag{2.2}$$

where κ and σ are the bending moduli and the surface tension of the membrane, respectively. In our notation, κ has units of energy, and σ is represented in units of energy per area. The *free* part of the membrane is parametrized by the arclength s. Using the Helfrich energy, one can find the elastic energy per unit length of the *free* part as [10]

$$E_{\mathrm{free}} = 2\times\int_0^S \mathrm{d}s\left[\frac{\kappa}{2}\dot{\psi}^2 + \sigma(1-\cos\psi)\right], \tag{2.3}$$

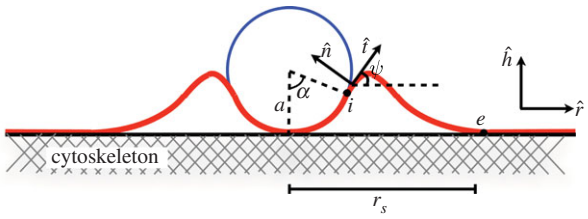

Figure 1. The schematic picture of the cylindrical object adhered to the membrane, which is attached to the cytoskeleton. (Online version in colour.)

where the angle $\psi(s)$ represents the angle between the tangent vector of the membrane at point s with respect to the horizontal line, S denotes the total contour length of the *free* part and the 'dot' indicates a derivative with respect to the arclength s. The integral term has been multiplied by 2 for considering the whole free part of the membrane, say in the left and right of the cylinder. Note that E_{free} in equation (2.3) is an energy difference wherein energy of the flat membrane ($\psi = 0$) has been subtracted.

For further calculations, it is convenient to write the energy contributions in the dimensionless manner using the bending constant κ and the radius of the cylinder a. First, we define the following dimensionless variables

$$\bar{w} \equiv \frac{2wa^2}{\kappa};\quad \bar{w}_s \equiv \frac{2w_s a^2}{\kappa};\quad \bar{\sigma} \equiv \frac{2\sigma a^2}{\kappa} \tag{2.4}$$

and $$\bar{E}_{\mathrm{free}} \equiv \frac{E_{\mathrm{free}} a}{\kappa}.$$

Using the mentioned variables, the dimensionless total energy of the problem, $\bar{E} \equiv Ea/\kappa$, can be written as

$$\bar{E} = -\bar{w}\alpha + \bar{w}_s\frac{r_s}{a} + \alpha + \bar{\sigma}\alpha\left(1 - \frac{\sin\alpha}{\alpha}\right) + \bar{E}_{\mathrm{free}}. \tag{2.5}$$

Minimizing the equation (2.5) with respect to α gives the equilibrium shape of the colloid–membrane system. The minimization of the integral term, $\bar{E}_{\mathrm{free}}$, can be done using the Hamiltonian equations, as is seen below.

2.1. Shape equations of the free membrane

The energy functional of the free part of the membrane can be written as

$$\bar{E}_{\mathrm{free}} = \int_0^s \mathrm{d}s\,\mathscr{L}(\psi,\ \dot{\psi},\ \dot{h},\ \dot{r},\ \lambda_h,\ \lambda_r), \tag{2.6}$$

where $\mathscr{L}$ denotes the Lagrangian of the problem and is given [3,13,16]

$$\mathscr{L} = \frac{a}{2}\dot{\psi}^2 + \frac{\bar{\sigma}}{2a}(1-\cos\psi) - \lambda_r(\dot{r} - \cos\psi) - \lambda_h(\dot{h} - \sin\psi). \tag{2.7}$$

The two first terms include the bending and tension energy of the membrane, whereas $\lambda_r(s)$ and $\lambda_h(s)$ are the Lagrange multiplier functions to guarantee the geometrical relations of $\dot{r} = \cos\psi$ and $\dot{h} = \sin\psi$, respectively. It is convenient to use the Hamiltonian formalism to determine the shape of the membrane. We use the same procedure discussed in reference [13] and obtained the following Hamiltonian

$$\mathscr{H} = \frac{p_\psi^2}{2a} - \frac{\bar{\sigma}}{2a}(1-\cos\psi) + p_r\cos\psi + p_h\sin\psi, \tag{2.8}$$

where p_q denotes the momentum conjugate of the generalized coordinate q. Now, one can use the Hamiltonian equations in

order to find the shape equations as

$$\dot{h} = \sin\psi, \tag{2.9a}$$

$$\dot{r} = \cos\psi, \tag{2.9b}$$

$$\dot{\psi} = \frac{p_\psi}{a}, \tag{2.9c}$$

$$\dot{p}_\psi = \left(\frac{\bar{\sigma}}{2a} + p_r\right)\sin\psi - p_h\cos\psi, \tag{2.9d}$$

$$\dot{p}_r = 0 \tag{2.9e}$$

and

$$\dot{p}_h = 0. \tag{2.9f}$$

According to equations (2.9*e*) and (2.9*f*), p_h and p_r are independent of s and thus are constant. We show that the vertical and horizontal components of the force acting on the membrane are proportional to p_h and p_r, respectively. The constant values of mentioned generalized momentum imply the equilibrium condition for the free part of the membrane. These equations can be solved numerically using proper boundary conditions, which is discussed in §3.

2.2. Derivation of the force

In order to find the force acting on the deformed membrane, we consider a membrane in such a way that its shape has been changed through the application of the force. Figure 2 shows the schematic picture of the deformed membrane.

We assume a very long cylinder and invariance by translation along the cylinder axis. It is thus sufficient to define one tangent vector at each point as $\hat{t}(s) \equiv \partial_s \boldsymbol{r}(s)$, where ∂_s denotes the derivative with respect to s and $\boldsymbol{r}(s)$ parametrizes the position on the surface of the membrane. Furthermore, we have

$$\partial_s \hat{t}(s) = -C(s)\hat{n}(s) \equiv \boldsymbol{C}, \tag{2.10}$$

where $C(s)$ and $\hat{n}(s)$ are the local curvature and the normal vector of the surface, respectively. For example for the bound membrane, if the normal vector of the surface is pointing outwards, the curvature C is defined negative. Owing to the deformation, the tangent vector, $\hat{t}(s)$ and the local curvature, $\boldsymbol{C}(s)$, are changed to $\hat{t} + \delta\hat{t}$ and $\boldsymbol{C} + \delta\boldsymbol{C}$. After some manipulation, one finds

$$\delta\hat{t} = [\partial_s(\delta\boldsymbol{r}) \cdot \hat{n}]\hat{n}, \tag{2.11}$$

and

$$\delta\boldsymbol{C} = 2C[\partial_s(\delta\boldsymbol{r}) \cdot \hat{t}]\hat{n} + C[\partial_s(\delta\boldsymbol{r}) \cdot \hat{n}]\hat{t} + [\partial_{s,s}(\delta\boldsymbol{r}) \cdot \hat{n}]\hat{n}, \tag{2.12}$$

where $\partial_{s,s} \equiv \partial^2/\partial s^2$.

The energy difference of the free part of a membrane with respect to a flat membrane in a general form can be written as

$$E = \int ds\left[\frac{1}{2}\kappa C^2 + \sigma(1 - \hat{t}\cdot\hat{r})\right], \tag{2.13}$$

and

$$E + \delta E = \int ds'\left[\frac{1}{2}\kappa(\boldsymbol{C} + \delta\boldsymbol{C})^2 + \sigma[1 - (\hat{t} + \delta\hat{t})\cdot\hat{r}]\right], \tag{2.14}$$

where we have $ds' = ds[1 + \hat{t}\cdot\partial_s(\delta\boldsymbol{r})]$. It is worth mentioning that using $C = -\dot{\psi}$ and $\hat{t}\cdot\hat{r} = \cos\psi$, equations (2.13) and (2.14) recover the equation (2.3). After some calculations, the variation of the energy of the free part of the membrane gives

$$\delta E = -ds\mathscr{F}\cdot\partial_s(\delta\boldsymbol{r}), \tag{2.15}$$

where $\mathscr{F}$ is the force (per unit cylinder length) acting on the membrane that is associated with the deformation $\delta\boldsymbol{r}$. After a few calculations, $\mathscr{F}$ can be determined as

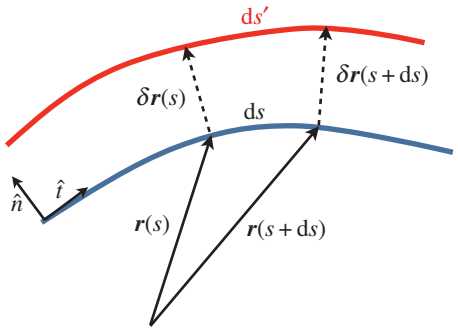

Figure 2. The schematic picture of the deformed membrane. The position of the membrane is given by the vector $\boldsymbol{r}(s)$ at point s, whereas the deformation vector is denoted by $\delta\boldsymbol{r}(s)$ at point s. In general, the length of a deformed part can be changed, e.g. ds is changed to ds'. (Online version in colour.)

$$\mathscr{F}(s) = \left[\frac{1}{2}\kappa[C(s)]^2 - \sigma(1 - \cos\psi)\right]\hat{t}(s) - [\kappa[\partial_s C(s)] + \sigma\sin\psi]\hat{n}(s). \tag{2.16}$$

We note that because we have subtracted the energy of the flat membrane (only tension energy) from the membrane Helfrich energy, the resulting force would be the 'force difference'. This relation in terms of the angle $\psi(s)$ is written as

$$\mathscr{F}(s) = \left[\frac{1}{2}\kappa\dot{\psi}^2 - \sigma(1 - \cos\psi)\right]\hat{t}(s) + [\kappa\ddot{\psi} - \sigma\sin\psi]\hat{n}(s). \tag{2.17}$$

Let us say a few words about the force acting on the membrane. One can consider a line parallel to the axis of the cylinder on the membrane. This hypothetical line divides the membrane into two sections, say left and right sections. The force acting on the left section from the right section of the membrane is denoted by $\mathscr{F}$. At equilibrium, the total force acting on each element of the membrane should be zero which means that $\partial_s\mathscr{F} = 0$. It implies that the force per unit length, $\mathscr{F}$, should not depend on s and is constant. Let us denote the components of the force along the coordinates as $\mathscr{F}_r \equiv \mathscr{F}\cdot\hat{r}$ and $\mathscr{F}_h \equiv \mathscr{F}\cdot\hat{z}$. Using these components, one can easily see that

$$\frac{\kappa}{2}\dot{\psi}^2 - \sigma(1 - \cos\psi) = \mathscr{F}_r\cos\psi + \mathscr{F}_h\sin\psi. \tag{2.18}$$

After defining $p_r \equiv -\mathscr{F}_r a/\kappa$, $p_h \equiv -\mathscr{F}_h a/\kappa$, and obtaining derivative equation (2.18) respect to s, we can find the shape equation of the membrane. Therefore, the Lagrange multipliers of p_h and p_r, associated with the constraints of equations (2.9*a*) and (2.9*b*), are proportional to the vertical and horizontal force acting on the membrane [17].

2.3. The adhesion and the membrane contact curvature

Membrane binding to an external object imposes constraints on the free membrane shape. It can be shown that [13,18]

$$\dot{\psi}_\mathrm{i} = C_\mathrm{ob} - \frac{1}{a}\sqrt{\bar{w}} \quad \text{and} \quad \dot{\psi}_\mathrm{e} = \frac{1}{a}\sqrt{\bar{w}_s}, \tag{2.19}$$

where the indices 'i' and 'e' refer to the initial and endpoints of the free membrane (figure 1), and where C_ob denotes the curvature of the object.

It is worth mentioning that the equations (2.19) are found using the proper variational method and in principle are

independent. Therefore, one can consider them separately in determination of the shape of the membrane in the problem.

2.4. Boundary conditions

In order to find the shape of the membrane and the amount of engulfment of the object by the membrane, we need to know the proper boundary conditions of the system. In our problem, the membrane engulfs the cylindrical object by the amount of α. Therefore, according to figure 1, one has

$$r_{\mathrm{i}} = a\sin\alpha, \tag{2.20a}$$

$$h_{\mathrm{i}} = a(1-\cos\alpha) \tag{2.20b}$$

and

$$\psi_{\mathrm{i}} = \alpha, \tag{2.20c}$$

At the endpoint of the free membrane, we have two more boundary conditions as

$$\psi_{\mathrm{e}} = 0 \tag{2.21}$$

and

$$h_{\mathrm{e}} = 0. \tag{2.22}$$

There is another boundary condition that we should consider. Because we are dealing with the equilibrium, the final boundary condition should involve the force balance. This very important condition, which fulfills the force balance requirement of the free membrane in the equilibrium, can be found using (2.18) to find the $p_{\psi_{\mathrm{i}}}$ as

$$p_{\psi_{\mathrm{i}}} = -[\bar{\sigma}(1-\cos\alpha) - 2a(p_r\cos\alpha + p_h\sin\alpha)]^{1/2}, \tag{2.23}$$

where we have used this fact that through the free membrane p_r and p_h are constants, as can be seen in equations (2.9*e*) and (2.9*f*). Because at the point where the membrane leaves the cylindrical object, $\dot{\psi}_{\mathrm{i}}$ and hence $p_{\psi_{\mathrm{i}}}$ are negative, the minus sign has been used in the above relation to ensure this requirement.

2.5. Adhesion forces

As we discussed above, one can find the force acting on the membrane using equation (2.17) or equation (2.18). Because the force is constant through the deformed membrane, it is convenient to find the force components at the end of the free membrane. At r_s, we have $\psi_{\mathrm{e}}= 0$ and using the equation (2.18) at this point gives

$$\frac{\mathscr{F}_r}{\mathscr{F}_0} = \bar{w}_s\,, \tag{2.24}$$

where $\mathscr{F}_0 \equiv \kappa/(2a^2)$. According to equation (2.24), the horizontal component of the force is given by $\bar{w}_s \times \mathscr{F}_0 = w_s$ and it does not explicitly depend on the other physical parameters of the problem.

The vertical component of the force on the object can be obtained using the force equation (2.18) with the boundary conditions, equations (2.19) and (2.20*c*)

$$\frac{\mathscr{F}_h}{\mathscr{F}_0} = \frac{1}{\sin\alpha}\left[(1-\sqrt{\bar{w}})^2 - \bar{\sigma}(1-cos\alpha) - \bar{w}_s\, cos\alpha\right]. \tag{2.25}$$

3. Results

As mentioned above, the shape equations of the membrane are nonlinear differential equations. To study the effect of various parameters, namely the membrane bending rigidity and the surface tension, the radius of the object, the membrane–object and the membrane–substrate adhesion energy, we choose to work with the dimensionless parameters $\bar{\sigma}$, $\bar{w}$ and $\bar{w}_s$, as defined in equation (2.4).

In the following sections, we solve the set of coupled nonlinear equations of (2.9*a–f*) numerically for the different values of contour length of the free membrane, S, and the proper boundary conditions as discussed before. We calculate the phase diagram of membrane wrapping in the parameter space $\{\bar{w},\ \bar{w}_s\}$, which contains unwrapped, partially wrapped and fully wrapped regions. We then discuss the value of the wrapping angle, the extent of the membrane region detached from the cytoskeleton and the normal force on the target for different values of the parameters. Finally, we give analytical results for small and large wrapping angles that yield analytical expressions for the unwrapping and full wrapping boundaries of the phase diagram.

3.1. Numerical results

To study the effect of the membrane–object and the membrane–substrate adhesion energies on the engulfment angle, we solve the problem numerically with different parameters. The results are summarized in figure 3*a*, where a diagram in the parameter space of $\bar{w}$ and $\bar{w}_s$ shows the different wrapping regimes. Generally, there are three distinct regions. For small values of the membrane–cylinder adhesion $\bar{w}$, the engulfment angle is zero, which means that the membrane–substrate adhesion completely abolishes membrane wrapping around the cylinder. This region called U. Beyond a finite value of $\bar{w}$, the membrane deforms and partially unglues the target. This partially wrapped region is denoted by P. For sufficiently large values of $\bar{w}$, the membrane is fully wrapped around the cylinder (region F). Figure 3*b* shows the variation of the wrapping angle with the target binding energy, which clearly shows the existence of an abrupt transition to full wrapping for a finite binding energy. The shape of the free membrane is shown in figure 3*c*. For strong wrapping, the membrane away from both the target and the cytoskeleton shows a curvature-free straight shape characteristic of a cylindrical symmetry.

In figure 4, the dependence of the engulfment angle α, the distance r_s/a over which the membrane is detached from the cytoskeleton, and the vertical force $\mathscr{F}_h$ are shown as a function of $\bar{w}_s$ for different values of $\bar{\sigma}$ (for $\bar{w} = 200$). As expected, the binding energy between the membrane and the cortex can regulate the extent of wrapping. Increasing w_s decreases both the wrapping angle α and the detached length r_s. On the other hand, the normal force exerted by the target on the cell is a monotonously increasing function of w_s.

3.2. Analytical derivation of the phase boundaries

For sufficiently small values of the cytoskeleton binding energy w_s, the transition between the unwrapped and wrapped membrane states is continuous and can be derived analytically by performing a small angle expansion of the equations. It is shown in the appendix that for small α, the energy of the system given by equation (2.5) takes the form

$$\bar{E} = A_1(\bar{w},\ \bar{w}_s)\alpha - A_2(\bar{w},\ \bar{w}_s\,,\ \bar{\sigma})\alpha^3. \tag{3.1}$$

predicting an equilibrium wrapping angle $\alpha = \sqrt{-(A_1)/(3A_2)}$, and a wrapping transition for a value w_u of the target binding

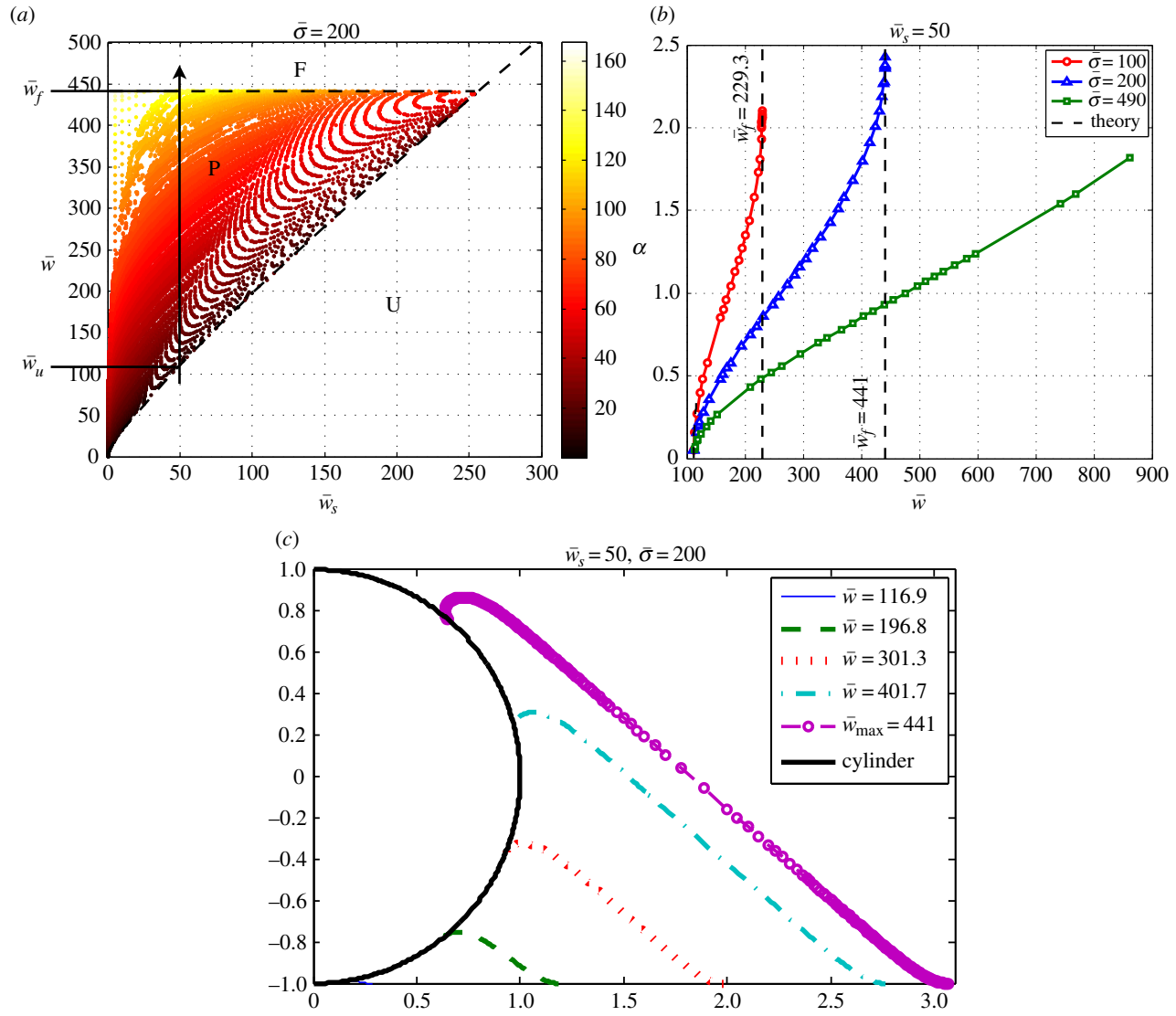

Figure 3. (*a*) The phase space of the engulfment of the cylindrical object (for $\bar{\sigma} = 200$) showing the different wrapping regimes in the parameter space of $\{\bar{w}, \bar{w}_s\}$. The colour bar in the right panel shows different colours corresponding to the engulfment angle, which is shown in degrees. The letters F, P, and U stand for fully wrapped, partially wrapped and unwrapped, respectively. The dashed lines show the analytical boundaries discussed in §3.2. (*b*) Variation of the wrapping angle α with $\bar{w}$ for different values of $\bar{\sigma}$. Plot (*a*) corresponds to the line with triangles. The analytical results for small and large wrapping are shown as dashed lines. (*c*) Plot of the membrane shape for increasing target binding energy $\bar{w}$, following the vertical arrow in (*a*). (Online version in colour.)

energy satisfying $A_1(\bar{w}_u, \bar{w}_s) = 0$, which implies

$$\bar{w}_u = \left(1 + \sqrt{\bar{w}_s}\right)^2 + \frac{4}{9}\left[\left(1 + 3\sqrt{\bar{w}_s}\right)^{3/2} - 1\right]. \tag{3.2}$$

This relation corresponds to the dashed line that separates the unwrapping region from the partially wrapping region in figure 3*a*. In the limit $\bar{w}_s \gg 1$, one finds $\bar{w}_u \simeq \bar{w}_s$.

The transition to full wrapping that occurs for large values of the target binding energy can be understood by looking at the variation of the wrapping angle α with $\bar{w}$ and the behaviour of the horizontal component of force, $\mathscr{F}_h$, in terms of α. As can be seen in figure 3*b*, α increases with w and at some point it diverges, which means $\partial\bar{w}/\partial\alpha = 0$ at the divergence point. Furthermore, as figure 5*a* shows, $|\mathscr{F}_h|$ decreases with α and becomes constant for large enough wrapping angle, that implies $\partial\mathscr{F}_h/\partial\alpha = 0$ for large values of α. Using these two criteria and after taking a derivative of equation (2.25) with respect to α at constant values of $\bar{\sigma}$ and $\bar{w}_s$, one finds

$$\frac{\mathscr{F}_h^*}{\mathscr{F}_0} = (\bar{w}_s - \bar{\sigma})\tan\alpha, \tag{3.3}$$

where $\mathscr{F}_h^*$ denotes the value that the vertical force converges to that at large α (figure 5*a*).

In addition as discussed in the §2.2, at the equilibrium, the force is constant through the contour length of the membrane. In figure 5*b*, the behaviour of ψ is shown in terms of the contour length. As can be seen in figure 5*b*, there is an area in which the angle ψ is constant, say ψ_0, that implies $\dot{\psi}|_{\psi_0} = 0$ and $\ddot{\psi}|_{\psi_0} = 0$. Therefore, the force components can be written in terms of ψ_0 as $\mathscr{F}_h = -\sigma\sin\psi_0$ and $\mathscr{F}_r = \sigma(1 - \cos\psi_0)$. Because $\sin^2\psi_0 + \cos^2\psi_0 = 1$, we can find the relation between the components of the force as $\mathscr{F}_h^2 = \sigma^2 - (\mathscr{F}_r - \sigma)^2$. Using equation (2.24) and after a few manipulations, we have

$$\left(\frac{\mathscr{F}_h}{\mathscr{F}_0}\right)^2 = \bar{w}_s(2\bar{\sigma} - \bar{w}_s). \tag{3.4}$$

This relation is also valid for large values of wrapping angle. After using equations (3.3) and (3.4), one can find the following relation for angle α_f at the fully wrapped transition

$$\cos\alpha_f = \frac{\bar{w}_s - \bar{\sigma}}{\bar{\sigma}}. \tag{3.5}$$

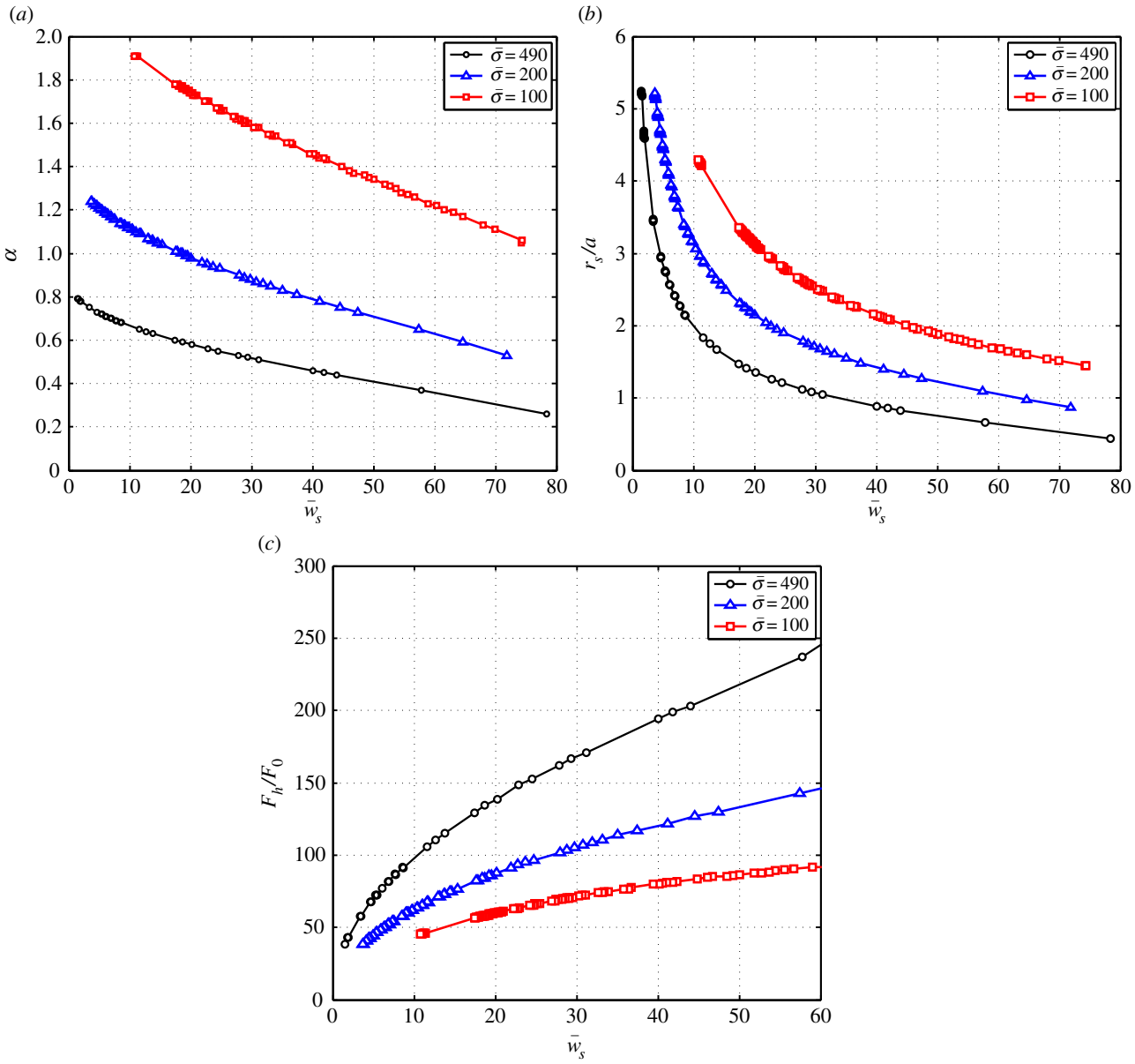

Figure 4. (*a*) The engulfment angle, α, and (*b*) the distance r_s/a as functions of membrane–substrate adhesion, $\bar{w}_s$. The plots correspond to $\bar{w} = 200$. The circles correspond to $\bar{\sigma} = 490$, the triangles correspond to $\bar{\sigma} = 200$ and the squares correspond to $\bar{\sigma} = 100$. (*c*) The vertical force, $\mathscr{F}_h$, acting on the membrane at r_i as a function of membrane–substrate adhesion, $\bar{w}_s$, for $\bar{w} = 200$. (Online version in colour.)

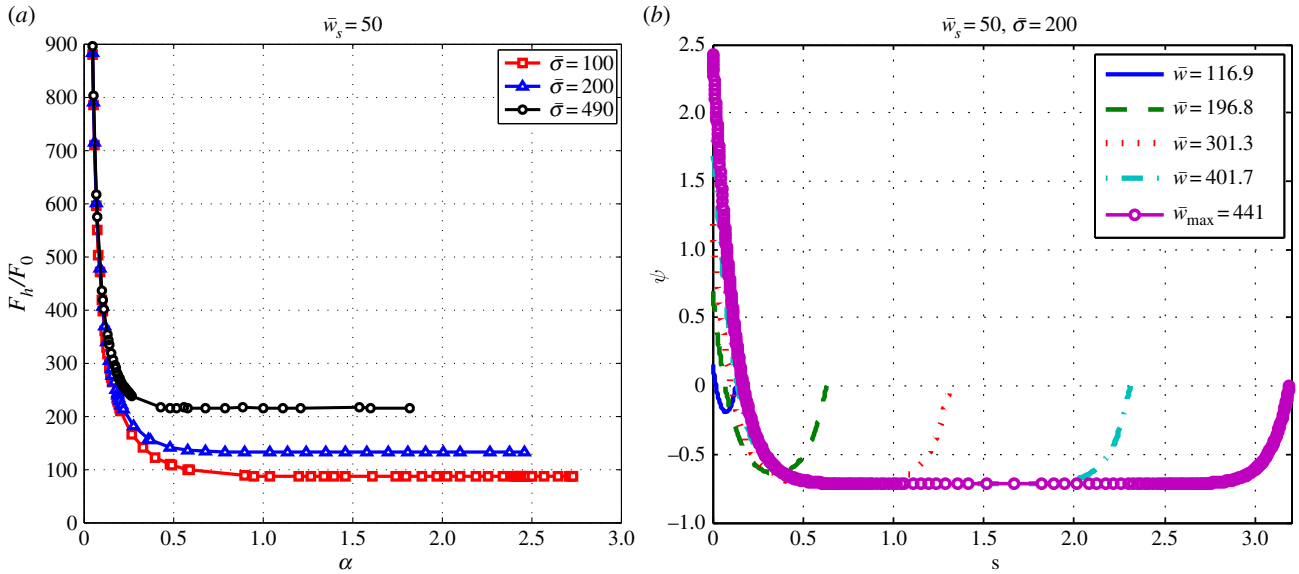

Figure 5. (*a*) The vertical force, $\mathscr{F}_h$, as a function of the engulfment angle, α, for different values of $\bar{\sigma}$ and $\bar{w}_s = 50$. (*b*) The behaviour of the local angle, ψ, at point s for $\bar{w}_s = 50$, $\bar{\sigma} = 200$, and different values of $\bar{w}$. (Online version in colour.)

After using the above relation, equations (2.25) and (3.3), we find the relation for the transition to full wrapping that occurs beyond a threshold for the membrane–target binding energy, $\bar{w}_\mathrm{f}$ as

$$\bar{w}_\mathrm{f} = \left(1 + \sqrt{2\bar{\sigma}}\right)^2. \tag{3.6}$$

This criterion is shown in figure 3 to give an accurate prediction of the critical target binding energy beyond which one expects full wrapping.

One can see in figure 3*a* that the full wrapping boundary is by and large independent of $\bar{w}_\mathrm{s}$. One thus expect $\bar{w}_f \propto \bar{\sigma}$, and considering the deformed membrane contains two membrane sheets (each experiencing a force $\sim \bar{\sigma}$), but only one of them experiences the driving force $\bar{w}$, one expects $\bar{w}_\mathrm{f} \simeq 2\bar{\sigma}$. This criterion is shown in figure 3 to give an accurate prediction of the critical target binding energy beyond which one expects full wrapping.

The boundary lines defining the partially wrapped state intersect when $\bar{w}_s = 2\bar{\sigma}$. The boundary lines defining the partially wrapped state are of interest when $\bar{w}_f$ (equation (3.6)) equals $\bar{w}_u$ (equation (3.2)). In the limit of negligible bending rigidity, this corresponds to $\bar{w}_s \simeq 2\bar{\sigma}$. For larger binding energies, the partially wrapped state does not exist. One then expects to observe an abrupt transition from an unwrapped to a fully wrapped state when $\bar{w}$ becomes larger than $\bar{w}_s$.

4. Discussion and conclusion

In this paper, we have studied the engulfment of a cylindrical object by a bilayer adhering on a rigid plane. This problem gives insights into the competition between membrane–target and membrane–cytoskeleton adhesion in cellular processes such as phagocytosis and viral infection. We examined several physical parameters such as the membrane–object adhesion, the membrane–surface adhesion, the bending stiffness and the surface tension of the membrane. We have summarized the effect of all mentioned parameters in the phase space of the engulfment in figure 3. The most striking features of the phase space is the existence of three well-defined regions: unwrapped, partially wrapped and fully wrapped. In other words, no wrapping is observed for a target adhesion energy $\bar{w} < \bar{w}_\mathrm{u}$ and full wrapping is predicted for $\bar{w} > \bar{w}_\mathrm{f}$, where $\bar{w}_\mathrm{u}$ and $\bar{w}_\mathrm{f}$ are functions of the cytoskeleton adhesion energy, the membrane tension and the bending rigidity, and the radius of the object for which we give analytical expressions (equations (3.2) and (3.6)). Although cellular processes such as phagocytosis involve active force generation by the cytoskeleton in addition to specific adhesion, the former is often triggered by the later [19]. The existence of an unwrapping transition of $\bar{w} < \bar{w}_\mathrm{u}$ is thus of strong physiological relevance. The cell is not able to establish any sort of extended contact with the target if the cytoskeleton binding energy is above the threshold. Factors that affect the tightness of the cytoskeleton anchoring to the plasma membrane might thus serve as crucial regulators of the cell's ability to recognize external objects. Note that the value of $\bar{w}_\mathrm{u}$ is influenced by the bending rigidity of the cell membrane, but not by the cell membrane tension.

One consequence of the abrupt nature of the fully wrapped transition is that there is a maximum partial wrapping angle α_f (given by equation (3.5)), which is modulated by membrane tension. At equilibrium, the wrapping angle is either below α_f or equal to π (full wrapping). This result could help explain the experimental observation that phagocytic cups are either stalled at small wrapping angle or they progress until the target of phagocytosis is fully engulfed by the cell [20]. It was argued in [20] that the critical angle must by $\pi/2$, based on a crude model of the membrane deformation energy. We show here that both the membrane–cytoskeleton adhesion energy and the membrane tension can regulate the critical cup size.

Our results are expressed in terms of reduced parameters, listed in equation (2.4). These parameters depend on the size of the object, which plays an important role in defining the accessible regions of the phase space (figure 3). For typical physiological values of membrane tensions and bending rigidity: $\sigma \simeq 10^{-6}$ to 10^{-3} N m^{-1} [21] and $\kappa \simeq 10 - 100, k_\mathrm{B}T$ [2], we find that $\bar{\sigma} = 10^{-1}$ to 10^3 for $a = 100$ nm, or $\bar{\sigma} = 10 - 10^5$ for $a = 1$ μm. The binding energies w and w_s can be expected to be on the order of several $k_\mathrm{B}T$ per adhesion site, or on the order of $\bar{w}$, $\bar{w}_s \sim 10 - 10^3$. This shows that (i) the physiological system can explore the entirety of the phase space, and (ii) physiological membrane tension can, in principle, regulate target wrapping. Note that the parameter values above are typical magnitudes of lipid bilayers without considering effects of the cell cortex, a thin (<μm) actin layer underlying the cell membrane.

Possible extensions of this work should include an analysis of the influence of the target geometry on the degree of wrapping. The local curvature of the object is important to fix the boundary condition (equation (2.19)), and can potentially control wrapping locally. Furthermore, as discussed above, the target size is crucial to fix the energy scales on locate the system in the phase space of figure 3. Another interesting extension is to consider the substrate on which the membrane adheres as a deformable object, such is the cytoskeleton. One could envision two main alterations of our present model. First, the effective substrate adhesion energy would probably be reduced, as an increase of the wrapping angle could be obtained either by detaching the membrane from the cytoskeleton or by deforming the cytoskeleton. Second, wrapping could be obtained by deforming the membrane upwards, or by bringing the target downwards–upwards. We plan to explore this more complex situation in the future.

Acknowledgement. We thank M. Deserno for very helpful discussions.
Funding statement. P.S. acknowledges financial support by the Human Frontier Science Programme under the grant no. RGP0058/2011.

Appendix A. Small angle expansion

Here, we try to understand the behaviour of the problem for small angles of engulfment analytically. For small values of α, let us say for $\alpha \ll 1$, $\dot{\psi}(s)$ behaves linearly in terms of s. We write this relation as

$$\dot{\psi}(s) = A + Bs, \tag{A 1}$$

where A and B are constants. We know $\dot{\psi}$ at r_i and r_s as

$$\dot{\psi}_i = \dot{\psi}(0) = \frac{1}{a}\left(1 - \sqrt{\bar{w}}\right) \tag{A 2}$$

and

$$\dot{\psi}_s = \dot{\psi}(S) = \frac{1}{a}\sqrt{\bar{w}_s}, \tag{A 3}$$

where S denotes the total contour length of the free part. Furthermore, one can find $\psi(s)$ by integrating equation (A 1). So one has

$$\psi(s) = As + \frac{1}{2}Bs^2 + C. \tag{A 4}$$

We have more two boundary conditions $\psi(0) = \alpha$ and $\psi(S) = 0$. Here, the unknown parameters or constants are A, B, C and S. Using equations (A 2)–(A 4), we have

$$A = \frac{1}{a}\left(1 - \sqrt{\bar{w}}\right), \tag{A 5}$$

$$BS = \frac{1}{a}\left(\sqrt{\bar{w}_s} - 1 + \sqrt{\bar{w}}\right), \tag{A 6}$$

$$C = \alpha \tag{A 7}$$

and

$$S = \frac{2a\,\alpha}{\sqrt{\bar{w}} - 1 - \sqrt{\bar{w}_s}}. \tag{A 8}$$

The total energy is given by

$$E = E_{\mathrm{cap}} + E_{\mathrm{ad}} + E_{\mathrm{free}}, \tag{A 9}$$

$$E_{\mathrm{cap}} = \kappa\frac{\alpha}{a} + 2\sigma\alpha a\left(1 - \frac{\sin\alpha}{\alpha}\right), \tag{A 10}$$

$$E_{\mathrm{ad}} = -2wa\alpha + 2w_s r_s \tag{A 11}$$

and

$$E_{\mathrm{free}} = 2 \times \int_0^S \mathrm{d}s\left[\frac{\kappa}{2}\dot{\psi}^2 + \sigma(1 - \cos\psi)\right], \tag{A 12}$$

where the factors '2' account for both sides of the cylinder. Using the dimensionless parameters, we have

$$\bar{E} = -\bar{w}\alpha + \bar{w}_s\frac{r_s}{a} + \alpha + \bar{\sigma}\alpha\left(1 - \frac{\sin\alpha}{\alpha}\right) + \bar{E}_{\mathrm{free}}\,. \tag{A 13}$$

We see that in the energy we need r_s. One can find r_s using the relation of $\dot{r} = \cos\psi$ as

$$r_s = a\sin\alpha + \int_0^S \cos\psi\,\mathrm{d}s. \tag{A 14}$$

As we are treating the small angle of α, therefore, in principle, ψ should also be small. We expand all the small angles to the third order. So, we can find r_s. Furthermore, we can calculate the energy of the free part, because we have $\psi(s)$ and $\dot{\psi}(s)$, and one can calculate the integral of the energy concerning of the free part. At the end, we find out the energy of the system as

$$\bar{E} = A_1(\bar{w},\ \bar{w}_s\,)\,\alpha + A_2(\bar{w},\ \bar{w}_s\,,\ \bar{\sigma})\,\alpha^3, \tag{A 15}$$

where $A_1(\bar{w},\ \bar{w}_s\,)$ and $A_2(\bar{w},\ \bar{w}_s\,,\ \sigma)$ are functions defined as

$$A_1(\bar{w},\ \bar{w}_s\,) = 3 - 2\sqrt{\bar{w}} - \bar{w} + \frac{8\left(-1 + \sqrt{\bar{w}}\right)^2}{3\left(-1 + \sqrt{\bar{w}} - \sqrt{\bar{w}_s}\right)} - \frac{8\sqrt{\bar{w}_s}}{3} + \bar{w}_s\,, \tag{A 16}$$

$$A_2(\bar{w},\ \bar{w}_s\,,\ \bar{\sigma}) = \frac{\bar{\sigma}}{6} + \frac{(\bar{\sigma} - \bar{w}_s\,) \times B(\bar{w},\ \bar{w}_s\,)}{5\left(-1 + \sqrt{\bar{w}} - \sqrt{\bar{w}_s}\right)} \tag{A 17}$$

and

$$B(\bar{w},\ \bar{w}_s\,) = 1 + \bar{w} - \sqrt{\bar{w}}\left(2 + 3\sqrt{\bar{w}_s}\right) + 3\sqrt{\bar{w}_s} + \frac{8}{3}\bar{w}_s\,. \tag{A 18}$$

In order to find α corresponding to the problem, we have to minimize the above energy with respect to α. We have

$$\frac{\partial\bar{E}}{\partial\alpha} = 0 \quad \Rightarrow \quad \alpha = \sqrt{\frac{-A_1}{3A_2}}. \tag{A 19}$$

To obtain the answer to the problem, the parameter $-A_1/(3A_2)$ should be positive. Using this criterion, one can find the boundary that can be seen in the phase diagram (figure 3*a*).

References

1. Alberts B, Johnson A, Lewis J, Raff M, Roberts K, Walter P. 2002 *Molecular biology of the cell*, 4th edn. New York, NY: Garland Science.
2. Lipowsky R, Sackmann E (eds). 1995 *Structure and dynamics of membranes*. Amsterdam, The Netherlands: Elsevier.
3. Seifert U. 1997 Configurations of fluid membranes and vesicles. *Adv. Phys.* **46**, 13–137 (doi:10.1080/00018739700101488)
4. Swanson JA. 2008 Shaping cups into phagosomes and macropinosomes. *Nat. Rev. Mol. Cell Biol.* **9**, 639–649. (doi:10.1038/nrm2447)
5. Bray D. 2001 *Cell movements: from molecules to motility*, 2nd edn. New York, NY: Garland Publishing.
6. Landau L, Lifshitz E. 1986 *Theory of elasticity*, 3rd edn. Oxford, UK: Pergamon.
7. Powers TR. 2010 Dynamics of filaments and membranes in a viscous fluid. *Rev. Mod. Phys.* **82**, 1607–1631. (doi:10.1103/revmodphys.82.1607)
8. Phillips R, Kondev J, Theriot J. 2009 *Physical biology of the cell*. New York, NY: Garland Science. Taylor & Francis.
9. Müller MM, Deserno M. 2005 Interface-mediated interactions between particles: a geometrical approach. *Phys. Rev. E* **72**, 061407. (doi:10.1103/PhysRevE.72.061407)
10. Helfrich W, Naturforsch Z. 1973 Elastic properties of lipid bilayers: theory and possible experiments. *Z. Nat. Teil C, Biochem. Biophys. Biol. Virol.* **28C**, 693–703.
11. Müller M, Katsov K, Schick M. 2006 Biological and synthetic membranes: what can be learned from a coarse-grained description? *Phys. Rep.* **434**, 113–176. (doi:10.1016/j.physrep.2006.08.003)
12. Mkrtchyan S, Ing C, Chen JZY. 2010 Adhesion of cylindrical colloids to the surface of a membrane. *Phys. Rev. E* **81**, 011904. (doi:10.1103/PhysRevE.81.011904)
13. Deserno M. 2004 Elastic deformation of a fluid membrane upon colloid binding. *Phys. Rev. E* **69**, 031903. (doi:10.1103/PhysRevE.69.031903)
14. Nicolas A, Geiger B, Safran SA. 2004 Cell mechanosensitivity controls the anisotropy of focal adhesions. *Proc. Natl Acad. Sci. USA* **101**, 12 520–12 525. (doi:10.1073/pnas.0403539101)
15. Safran SA, Gov N, Nicolas A, Schwartz US, Tlusty T. 2005 Physics of cell elasticity, shape and adhesion. *Physica A* **352**, 171–201. (doi:10.1016/j.physa.2004.12.035)
16. Jülicher F, Seifert U. 1994 Shape equations for axisymmetric vesicles: a clarification. *Phys. Rev. E* **49**, 4728. (doi:10.1103/PhysRevE.49.4728)
17. Castro-Villarreal P, Guven J. 2007 Axially symmetric membranes with polar tethers. *J. Phys. A, Math. Theor.* **40**, 4273. (doi:10.1088/1751-8113/40/16/002)
18. Fournier J-B. 2007 On the stress and torque tensors in fluid membranes. *Soft Matter* **3**, 883–888. (doi:10.1039/b701952a)
19. Groves E, Dart AE, Covarelli V, Caron E. 2008 Molecular mechanisms of phagocytic uptake in mammalian cells. *Cell. Mol. Life Sci.* **65**, 1957–1976. (doi:10.1007/s00018-008-7578-4)
20. van Zon JS, Tzircotis G, Caron E, Howard M. 2009 A mechanical bottleneck explains the variation in cup growth during FcγR phagocytosis. *Mol. Syst. Biol.* **5**, 298. (DOI:10.1038/msb.2009.59)
21. Morris CE, Homann U. 2001 Cell surface area regulation and membrane tension. *J. Membr. Biol.* **179**, 79–102. (doi:10.1007/s002320010040)